# VORTICITY DYNAMICS AND SYMMETRY BREAKING IN THE NEAR WAKE OF A FLAPPING FOIL

R. Godoy-Diana, C. Marais, J.-L. Aider & J. E. Wesfreid
*Physique et Mécanique des Milieux Hétérogènes*
*PMMH UMR7636 CNRS, ESPCI, Paris 6, Paris 7, Paris, France*

## ABSTRACT

*The vortex structures in the near wake of a flapping foil are studied using 2D Particle Image Velocimetry (PIV) from a hydrodynamic tunnel experiment. We study in particular the mechanisms that determine the symmetry breaking of the reverse Bénard-von Kármán vortex street and propose a semi-empirical model.*

## 1. INTRODUCTION

Flapping-based propulsive systems, either natural or man-made, are often discussed in terms of the Strouhal number, defined as the product of the flapping frequency $f$ and amplitude $A$ divided by the cruising speed $U$, i.e. $St_A = fA/U$ [Anderson et al., 1998, Taylor et al., 2003]. We have shown recently [Godoy-Diana et al., 2008] that the different regimes observed in the wake of the flapping foil, in particular the transition from a Bénard-von Kármán (BvK) vortex street to the reverse BvK street characteristic of propulsive regimes, and the symmetry breaking of the reverse BvK street, are better characterized using a two-parameter description, representing the frequency and amplitude of the oscillatory motion. The different observed regimes and in particular the transitions between them are summarized in the $(St, A_D)$ phase space shown in figure 1. The Strouhal number has been defined using a fixed length scale (the foil width $D$) as $St = fD/U$, and a dimensionless amplitude is defined as $A_D = A/D$.

In this paper we study in detail the spanwise vorticity field in the near wake of the flapping foil, relying on a hypothesis of quasi-two-dimensionality of the flow in the near wake owing to the high-aspect-ratio (4:1) of the foil. We focus especially on the reverse BvK regime attempting to shed some light on the physical mechanism that determines its symmetry breaking.

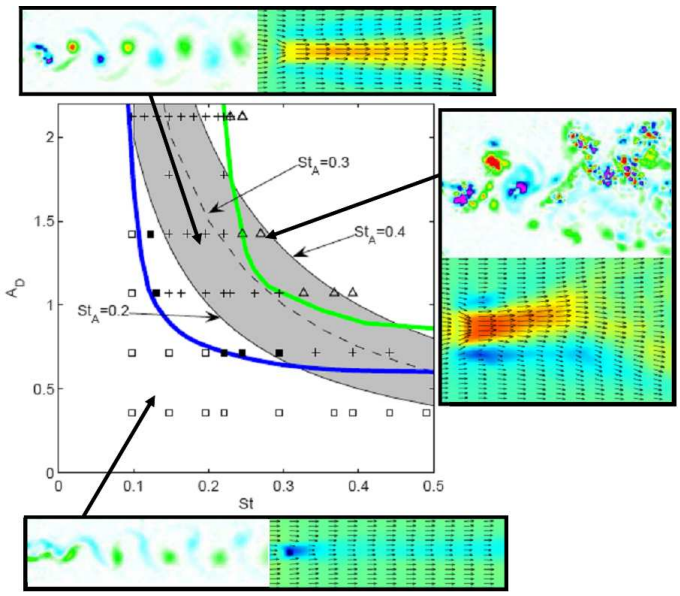


Figure 1: $A_D$ vs. St map for Re = 255 [from Godoy-Diana et al., 2008]. Experimental points are labeled as □: BvK wake; ■: aligned vortices (2S wake); +: reverse BvK wake; △: deflected reverse BvK street resulting in an asymmetric wake. Blue line: transition between BvK and reverse BvK. Green line: transition between reverse BvK and the asymmetric regime. Vorticity and mean horizontal velocity fields are shown for each regime.

## 2. EXPERIMENTAL SETUP

The setup is the same described in Godoy-Diana et al. [2008] and consists of a pitching foil placed in a hydrodynamic tunnel. The foil chord $c$ is 23mm and its span is 100mm which covers the whole height of the 100 × 150mm section of the tunnel. The foil profile is symmetric, opening at the leading edge as a semicircle of diameter $D = 5$mm which is also the maximum foil width. The pitching axis is driven by a stepper motor. The control parameters are the flow velocity in the tunnel $U$, the foil oscillation frequency $f$ and peak-to-peak amplitude $A$ which let us define the

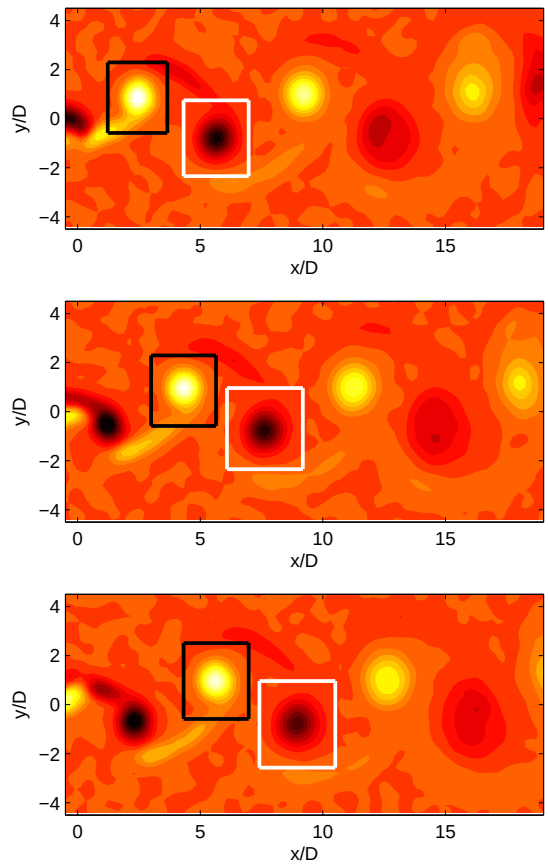


Figure 2: Vorticity fields in the wake of the flapping foil at $Re = 255$, $St = 0.15$ and $A_D = 1.42$.

Reynolds number, the Strouhal number and a dimensionless flapping amplitude as, respectively:

$$Re = UD/\nu \ , \quad St = fD/U \ , \quad A_D = A/D \ . \quad (1)$$

where $D$ is the foil width and $\nu$ is the kinematic viscosity. In the strongly forced regimes produced by the flapping foil, the flapping frequency used to define $St$ is equivalent to the main vortex shedding frequency. Measurements were performed using 2D Particle Image Velocimetry (PIV) on the horizontal mid-plane of the flap. PIV acquisition and post-processing was done using a LaVision system with an ImagerPro 1600 × 1200 12-bit CCD camera recording pairs of images at ∼ 15Hz and a two rod Nd:YAG (15mJ) pulsed laser. Laser sheet width was about 1mm in the whole 100mm × 80mm imaging region. The time lapse between the two frames (d$t$) was set to 12ms. Additional post-processing and analysis were done using Matlab and the PIVMat Toolbox [Moisy, 2007].

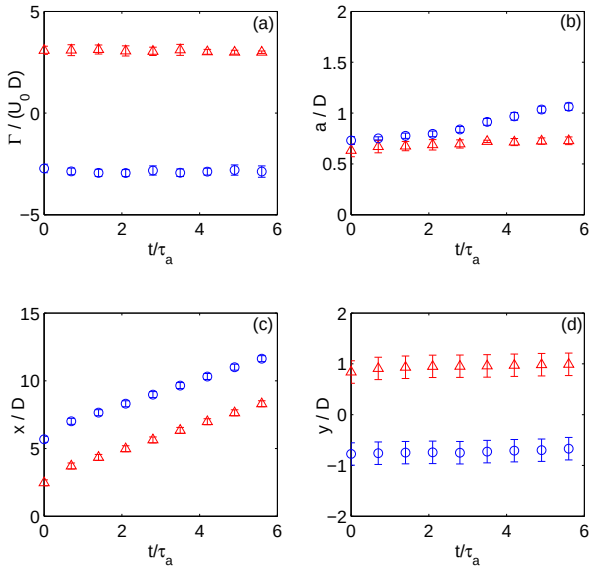


Figure 3: (a) Circulation (b) radius (c) $x$-position and (d) $y$-position of two consecutive (and counter-rotating) vortices in the wake of the flapping foil for the same parameters of figure 2.

## 3. OBSERVATIONS

### 3.1. The vorticity field

The $\omega_z$ vorticity field is calculated from the $u_x$ and $u_y$ fields obtained from PIV using 2nd-order centered differences. A sequence of vorticity fields of a reverse BvK street is shown in figure 2, where the position of two consecutive (and counter-rotating) vortices is followed using a search of local maxima and minima in the $\omega_z$ field.

### 3.2. The circulation Γ

An area of integration that encompasses each vortex needs to be defined in order to calculate its characteristic features such as circulation and size. We use gaussian fits $\exp(-x_i^2/\sigma^2)$ along the vertical and horizontal axes centered on the positions of the maxima and minima and define the sizes of the vortex along each direction $x$ and $y$ as $2\sigma$ (these are the horizontal and vertical sizes of the rectangles in the time sequence of figure 2). Since the vortex cores are nearly circular we define a single vortex radius $a$ as the mean of the sizes calculated along the two principal axes. The circulation Γ is then calculated either from a line integral of the velocity field or a surface integral of the vorticity field over each rectangle. Although in theory the two definitions of Γ are equivalent, the two calculations from the experimental fields

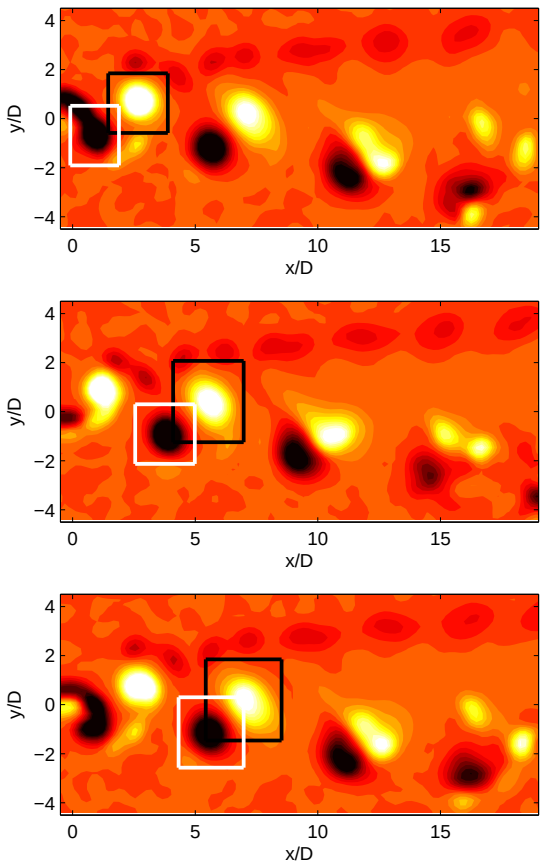


Figure 4: Vorticity fields in the wake of the flapping foil at $Re = 255$, $St = 0.27$ and $A_D = 1.42$.

are slightly different mainly because of the error induced by the finite-difference approximation of the vorticity. We use this difference to define the error bar in the circulation plotted in figure 3 where we also plot the time evolution of the vortices radii and positions.

### 3.3. The asymmetric wake

Figures 4 and 5 show the equivalent picture for an asymmetric wake. The Reynolds number and flapping amplitude are the same as in the case of the reverse BvK wake depicted in figures 2 and 3 and only the Strouhal number has been increased from 0.15 to 0.27. It can be readily seen that, although the algorithm for searching the vortex centers in the $\omega_z$ field works well, using the same definition of the area of interest for the calculation of the circulation will produce a slightly larger error because the vortices are too close of each other. This is evident from the time evolution of $\Gamma$ in figure 5.a, where the calculated value for the positive vortex decreases and then increases in time whereas a constant trend is observed for

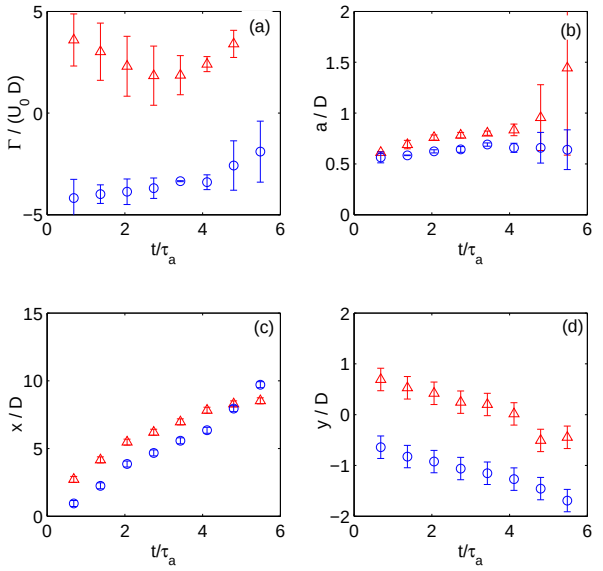


Figure 5: (a) Circulation (b) radius (c) $x$-position and (d) $y$-position of two consecutive (and counter-rotating) vortices in the wake of the flapping foil for the same parameters of figure 2.

the negative vortex. This spurious feature is due to having the region used for the circulation partially overlapping the neighboring vortex.

Concerning the calculation of the vortex size (figure 5.b), the estimation of the vortex radius also becomes noisier in the case of the asymmetric wake because of the deformation induced by the formation of a dipolar structure by the two counter-rotating vortices. On the other hand, the deflection of the wake is correctly captured by the time evolution of the $y$-coordinate in figure 5.d.

## 4. DISCUSSION

### 4.1. Back to the $(St, A_D)$ phase space

Thinking in a $(St, A_D)$ phase space perspective, we use the initial values of the circulation and the positions of the maxima and minima of $\omega_z$ in order to compare the vortices produced by different flapping configurations. We thus plot in figure 6 the initial value of the circulation as well as the distance between the two consecutive counter-rotating vortices as a function of $St$ for three series with different values of $A_D$. The main observation is that, for a given amplitude, the circulation increases and the distance between consecutive vortices decreases with increasing flapping frequency. Although this is not surprising, it is an important point because it lets us ascertain that a threshold curve determining the symmetry

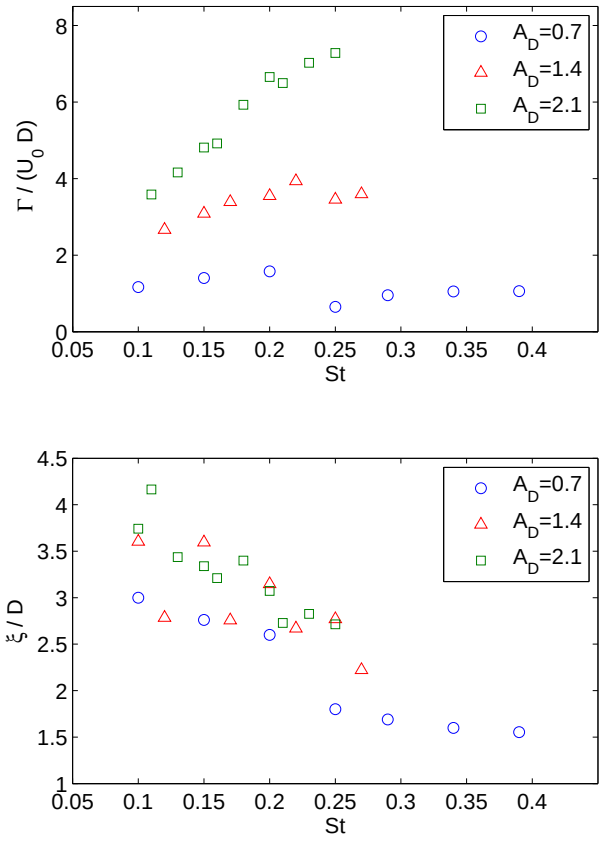


Figure 6: (a) Circulation $\Gamma$ and (b) distance between two consecutive vortices $\xi$ as a function of $St$ and $A_D$.

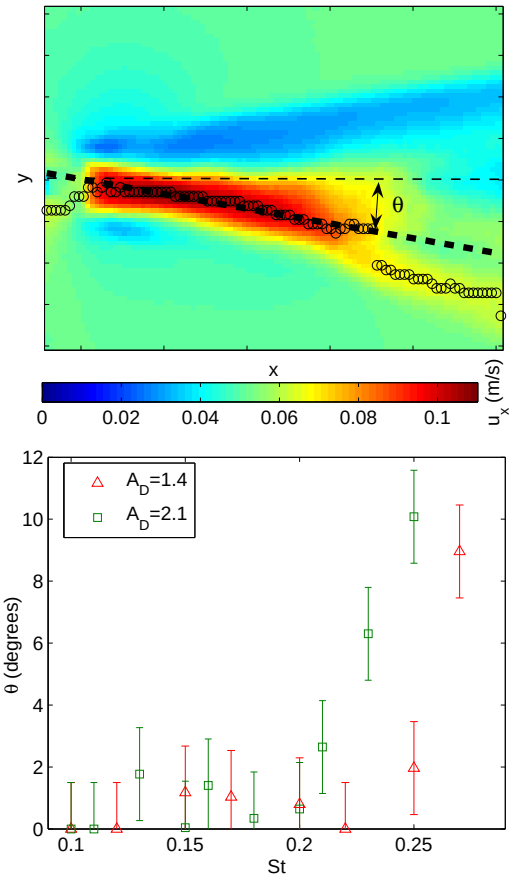


Figure 7: Definition of the asymmetry angle $\theta$ from the deflected mean jet flow (top) and $\theta$ as a function of the Strouhal number for $A_D = 1.4$ and 2.1 (bottom).

breaking of the reverse BvK wake can be traced in a $(\Gamma, \xi)$ space and also that a model containing the basic physics of the problem could be tested using experimental measurements.

### 4.2. Deflection angle of the asymmetric wake

The domain of existence of the reverse BvK vortex street is bounded on the upper-right zone of the $(St, A_D)$ phase space by a transition to an asymmetric regime (figure 1). In order to characterize this transition we define an angle of asymmetry $\theta$ using the direction of the jet observed in the mean velocity field (see figure 7). Of the three series with different flapping amplitudes presented in figure 6, the smallest one ($A_D = 0.7$) does not produce an asymmetric wake so only the cases of $A_D = 1.4$ and 2.1 are reported in figure 7. Although the data contain only a few points that correspond to asymmetric wakes, these are sufficient to show that the transition is rather abrupt and support the idea of the existence of a symmetry breaking threshold.

### 4.3. The dipole model

The physical mechanism giving rise to a deflected wake is based on the formation of a dipolar structure on each flapping period [Godoy-Diana et al., 2008], a feature that has also been observed in forced wakes in soap films [Couder and Basdevant, 1986], supporting the idea of a mainly 2D phenomenon. The initial condition sets the choice for the side where the asymmetry develops: the first dipole that is formed entrains fluid behind it, deflecting the mean flow in the wake and forcing the subsequent dipoles to follow the same path. This initial perturbation exists for all the $(St, A_D)$ parameter space, however, after a few periods of symmetric flapping motion, only in a region above a certain threshold (see figure 1) the wakes remain asymmetric.

The two quantities plotted in figure 6 can be used to give a measure of the strength of the dipolar structures that are formed for each flapping configuration. The simplest model that contains

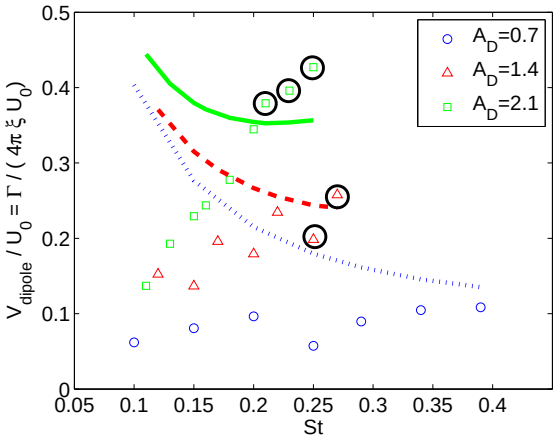


Figure 8: Translation speed of the initial dipoles calculated using Eq. 2 as a function of $St$ and $A_D$. The lines correspond to the semi-empirical model (dotted, dashed and solid lines correspond respectively to $A_D = 0.7, 1.4$ and $2.1$.

$\Gamma$ and $\xi$ is to consider a dipole made of two point vortices of circulations $\pm\Gamma$ separated by a distance $\xi$. In this case, the translation speed of the dipole (determined by the effect of each vortex over the other) is given by [see e.g. Saffman, 1992]

$$v_{\text{dipole}} = \frac{\Gamma}{2\pi\xi} \,. \tag{2}$$

The values of $v_{\text{dipole}}$ calculated using the data from figure 6 are shown in figure 8. As a direct consequence of the behavior of $\Gamma$ and $\xi$ in figure 6, for each flapping amplitude, the self-induced speed of the dipolar structure increases with the Strouhal number. It is remarkable that $v_{\text{dipole}}$ can reach values up to almost 50% of $U$. The experiments corresponding to asymmetric wakes are marked with a heavy circle in figure 8.

Clearly, attempting to define a threshold for the symmetry breaking solely depending on the value of $v_{\text{dipole}}$ would be overly simplistic. We propose a definition of a threshold function that depends directly on the distance between two consecutive vortices $\xi$ and the amplitude $A$ of the flapping motion (i.e. of the width of the wake), as well as inversely on the period of the flapping motion. In addition, the orientation of the dipolar structure (see the angle definition in figure 9) is also taken into account to ponder the effect of $v_{\text{dipole}}$. We thus define the threshold speed

$$v_{\text{T}} \propto \frac{\xi A_D}{T\cos\alpha} \,, \tag{3}$$

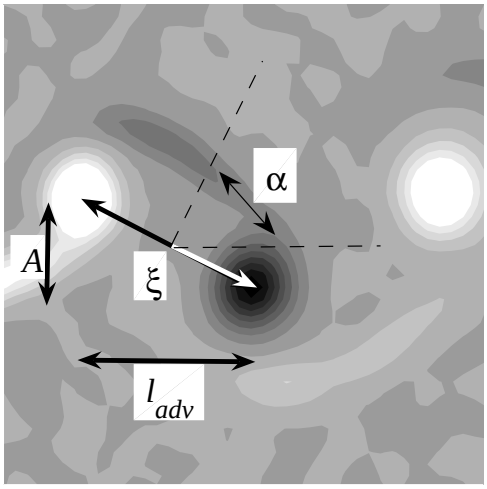


Figure 9: Definition of the angle $\alpha$ used in equation 3 using a triangle of sides $A$, $l_{adv}$ and $\xi$, where $l_{adv}$ is the advection length scale defined in **??**.

where $T$ is the flapping period and $\cos\alpha$ appears on the denominator to consider the projection of $v_{\text{dipole}}$ on the direction of the mean flow in the tunnel (the $x$ axis). We can rewrite the previous expression in terms of the Strouhal number and an advection time scale $\tau_{adv}$ and an arbitrary constant as

$$v_{\text{T}} = C\frac{\xi A_D St}{\tau_{adv}\cos\alpha} \,. \tag{4}$$

From figure 9, and approximating the advection length scale as the distance covered during half a flapping period at speed $U$, i.e.

$$l_{adv} \approx (T/2)U = D/2St \,, \tag{5}$$

it follows that

$$\alpha = \arctan\frac{l_{adv}}{A} = \arctan\frac{1}{2A_D St} \,, \tag{6}$$

which we have used to calculate the threshold curves $v_{\text{T}}$ plotted in figure 8. A single value of the arbitrary constant $C = 1/6$ was used for the three curves corresponding to different amplitudes, allowing for an acceptable estimation of the thresholds above which a symmetry breaking occurs.

## 5. CONCLUSIONS

We have proposed a mechanism for the symmetry breaking of the reverse Bénard-von Kármán

vortex street that has been observed in flapping-foil experiments [Jones et al., 1998, Godoy-Diana et al., 2008]and numerical simulations [Lewin and Haj-Hariri, 2003]. Analyzing PIV measurements from hydrodynamic tunnel experiments with a flapping foil, in particular the vorticity field in the near wake, we have built a semi-empirical model that allows to explain the symmetry breaking.

## 6. REFERENCES


J. M. Anderson, K. Streitlien, D. S. Barret, and M. S. Triantafyllou. Oscillating foils of high propulsive efficiency. *J. Fluid Mech.*, 360:41–72, 1998.

Y. Couder and C. Basdevant. Experimental and numerical study of vortex couples in two-dimensional flows. *J. Fluid Mech.*, 173:225–251, 1986.

R. Godoy-Diana, J. L. Aider, and J. E. Wesfreid. Transitions in the wake of a flapping foil. *Phys. Rev. E*, 77(1):016308, 2008.

K. D. Jones, C. M. Dohring, and M. F. Platzer. Experimental and computational investigation of the knoller-betz effect. *AIAA J.*, 36(7):1240–1246, 1998.

G. C. Lewin and H. Haj-Hariri. Modelling thrust generation of a two-dimensional heaving airfoil in a viscous flow. *J. Fluid Mech.*, 492:339–362, 2003.

F. Moisy. PIVMat: A PIV post-processing and data analysis toolbox for Matlab. Version 1.60 17-Apr-2007, 2007. URL `http://www.fast.u-psud.fr/pivmat/`.

P. G. Saffman. *Vortex Dynamics*. Cambridge University Press, 1992.

G. K. Taylor, R. L. Nudds, and A. L. R. Thomas. Flying and swimming animals cruise at a Strouhal number tuned for high power efficiency. *Nature*, 425:707–711, 2003.